International Journal of aeroacoustics volume 9 · number 4 & 5 · 2010 – pages 679–704

Plasma actuators for noise control

Xun Huang[1] and Xin Zhang[2]

[1]*Department of Mechanics and Aerospace Engineering, College of Engineering, Peking University, Beijing, China*

[2]*Airbus Noise Technology Centre, School of Engineering Sciences, University of Southampton, Southampton, UK*

In this article the use of plasma actuation for noise control is reviewed. This research follows the tradition of Geoffrey Lilley who conducted the first experiment relevant to aircraft noise, controlling jet noise by disrupting the helical mode of noise radiation. Advances in electronics, control theory, manufacture process, and diagnostic tools now allow more sophisticated control methods to be developed. In addition to propulsive system noise, airframe noise has now become equally important in defining the overall aircraft noise. Plasma actuation represents a novel method to control aircraft noise, worthy of research and development. Some advantages of the methods are simplicity, absence of mechanical moving parts, and fast response. Examples reviewed in this article demonstrated that the method can be used to attenuate both tonal and more importantly broadband noise radiated by components typically found on an aircraft. The limits and constraints of the methods are also discussed.

Key words: Plasma actuator, flow control, acoustic control, airframe noise

1. INTRODUCTION

1.1. Background

The aircraft noise problem was dominated by jet noise in the early days of civil aviation after the Second World War. Professor Geoffrey Lilley made a major contribution to aircraft noise study in the field of jet noise control. In 1952, Lilley and Westley conducted the first laboratory experiments in jet noise control, which was followed by Powell's study in 1953 at Southampton. The link between Geoffrey Lilley, Southampton, and noise control was a strong one. This was even more so when he moved to Southampton in 1964 as Professor and Head of the Department of Aeronautics and Astronautics. During his time as the head of department, he viewed experiments as a prominent area for the department with strong appointments and support. In 1988 he helped to move the 3.5 m by 2.7 m wind tunnel from then RAE Farnborough to Southampton with the aim of developing experimental aero-acoustic research. His design of low noise axial fan – he wrote the design code himself in Basic

language – is still being taught at the university. One of the authors of this article started his career at Southampton with Geoffrey Lilley working on an experimental project.

The way Geoffrey Lilley did his first experiments in jet noise control was a typical Lilley effort: he and Westley put a pencil (or their fingers) into the jet and therefore disrupted the helical modes and attenuated the noise radiation. Since these days, two major changes have occurred in the relevant field: a) experimental methods have become more sophisticated with development of electronics, control theory and diagnostic tools such as particle image velocimetry (PIV), microphone phase arrays, and novel approaches such as plasma actuators which will be the subject of this article, and b) aircraft noise problem has evolved significantly since the 1950s. Since the introduction of turbofan aero engines with bypass ducts, the role played by the airframe has become more prominent, especially at the approach-to-land phase of the aircraft operation. Airframe noise is now the focus of major studies in both the EU and the USA. This article introduces a method for flow and noise control using plasma actuation. Specifically we focus on the noise control aspect with discussions on actuator design, system requirement, and provide reviews of potential airframe noise control applications. Related research works, especially those previously conducted at the University of Southampton, are reviewed in this paper.

1.2. Plasma actuation

Plasma, operating in atmospheric pressure air conditions, offers potential to reduce flow-induced noise generated during the takeoff and approach-to-land of an aircraft (Raman & McLaughlin, 2000). The principle of using plasma actuators for aero-acoustic control is to sufficiently modify the flow field to disrupt or to alter the mechanisms of the generation of flow-induced noise. The advantages of using plasma actuators for flow and noise control include a) simplicity of systems and constructions and b) the absence of mechanical moving parts.

The principle of using plasma for flow and flow-induced sound control is not new. Plasma in the atmospheric pressure air mainly consists of charged nitrogen/oxygen particles. A plasma actuator is useful mainly for its physical properties, such as the induced body force by a strong electric field and the generation of heat during an electric arc. The recent invention of glow discharge plasma actuators by Roth (1998) that can produce sufficient quantities of glow discharge plasma in the atmosphere pressure air helps to yield an increase in flow control performance. The attention of this paper is therefore focused on the flow-induced sound control applications by glow discharges. Specifically, the flow adjacent to glow discharge plasma actuators can be maintained in a favorable state by a properly assigned electric force. The force is imposed on the partially ionized flow by the externally applied electric field between electrodes. The precise flow control physics under plasma actuation is still far from being understood and more research needs to be performed. However it is evident that the flow local to plasma actuators placed on an aerodynamic surface is altered, finally leading to global changes in the surrounding flow field.

In terms of flow control, some recent applications of plasma actuation include high-speed flow control using localized arc filament plasma actuators (Samimy *et al*., 2007a), surface impulse discharges (Gnemmi *et al*., 2008) and glow discharges (Elias *et al*.,

2007); flat plate boundary layer flow control by non-thermal direct current (DC) corona discharge (Moreau *et al*., 2006); airfoil separation control by glow discharge plasma actuators (Roth *et al*., 2000); and airfoil wake control by dielectric barrier discharge (DBD) plasma actuators (Greenblat *et al*., 2008).

These flow control methods using plasma actuators offer possibilities to control noise (without the need to physically change the shape of the aerodynamic surface) as flow and surface interaction represents one of the dominant sources of aerodynamic noise (Curle, 1955). Recent applications of acoustic control include cavity noise attenuation (Chan *et al*., 2007; Huang & Zhang, 2008), noise control model development (Huang *et al*., 2008a), and bluff body noise control (Huang *et al*., 2008b).

The paper is organized as follows. Section 2 briefly reviews the most recent designs of plasma actuators that are used in flow/noise control applications. Section 3 reviews some applications related to aero-acoustics, where plasma actuators are employed to control the flow and sound fields. Finally, section 4 summarizes the current state of research.

2. PLASMA ACTUATOR DESIGN AND SYSTEM

2.1. Principle of plasma actuation

A discharge generated between electrodes can take the form of continuous glow, periodic arc, or a momentary spark, mainly depending on the voltage drops between electrodes. Plasma actuators generally use the former two processes for flow control applications under atmospheric pressure. The main interest of this paper is on the control effect of flow-induced noise by plasma actuators that are able to generate weakly ionized atmospheric plasma, which is coupled to an electric field. Through Lorentzian collisions, momentum is transferred to the neutral gas from charged particles in the plasma, thus affecting the flow field local to the plasma actuator and subsequently facilitating flow and noise control applications. To generate atmospheric glow discharges in air, a sufficiently high potential is required to break down the surrounding species. The voltage potential is required at a kilohertz frequency to sustain the glow discharge. In addition, a dielectric barrier is used in some plasma actuator designs to prevent electron avalanches that lead to arcing, which produces a high temperature field. The intermittent inclusion of strong heat waves by arcing could be useful in flow control application as well. In brief, the fast control response, simplicity and absence of mechanical moving parts (e.g. pumps), make the plasma actuator a promising option.

2.2. Types of plasma actuator

Localized arc filament plasma actuators generate strong compression waves through rapid localized heating, which was presumed to act similarly to a sudden alternation of physical geometry (Leonov *et al*., 2003). This type of plasma actuators could produce strong arcing that is suitable for flow and subsequently noise control applications at high speed and high Reynolds number (Samimy *et al*., 2007a; Gnemmi *et al*., 2008; Utkin *et al*., 2007; Kim *et al*., 2009).

A localized arcing plasma system used for jet flow control is showed in Figure 1 following Samimy *et al*. (2007a), where eight plasma actuators are installed along the

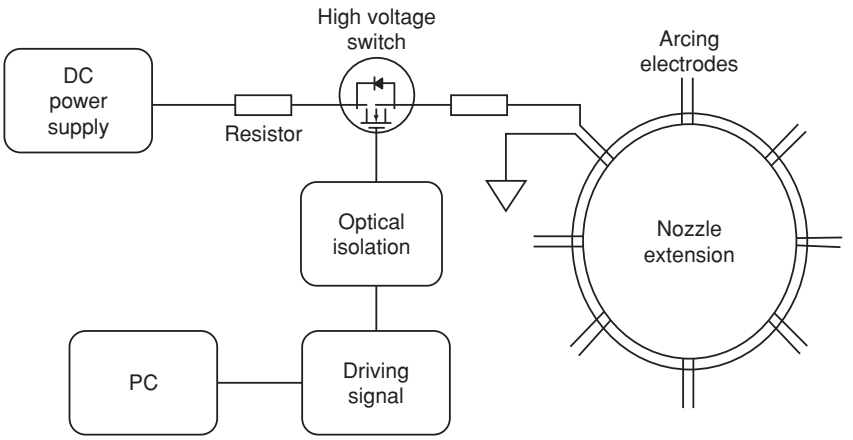

Figure 1: Schematic of a localised arcing plasma actuator system (Samimy *et al*., 2007a).

rim of a nozzle. Each actuator consists of two electrodes (spikes in Figure 1), one grounded, and the other connected to a high voltage DC power supply. The circuit for only one arcing actuator is displayed in Figure 1 for simplicity. A high voltage transistor switcher controls the activation duration for each actuator. When the transistor switcher is on, high DC voltage is applied on the connected electrode, from which to the grounded electrode a strong arcing appears. These localized arcing plasma actuators can be activated periodically. The duration of each actuation is generally in microsecond scale. The power consumption of each actuator is dozens of watts. The experiments showed that the jet flow and flow-induced noise can be controlled by exciting various modes with localized arcing. Similar ideas can trace back to earlier works of Morrison and McLaughlin (AIAA Journal, Vol 18, No. 7, pp. 793–800, 1980), and Stromberg *et al*., (Journal of Sound and Vibration, Vol 72, No. 2, 159–176, 1980)

Dielectric barrier discharge (DBD) actuators derive their names from that fact that a dielectric material is presented between electrodes to maintain glow discharge (Roth, 1998). Figure 2 shows a typical DBD plasma actuator system that includes a high voltage alternative current (AC) power supply and a plasma actuator (Huang *et al*., 2007). Any arcing produced between electrodes of a localized arcing actuator could be prevented in a DBD actuator by the dielectric material. As a result, glow discharges with a uniform distribution of plasma can be produced. Rather than inserting strong heat waves to the adjacent flow, DBD actuators control flow using non-thermal mechanisms. Through ionization the DBD plasma actuators generate weakly ionized atmospheric plasma that consists of charged particles, which are moved within the coupled electric field. Through collisions between the charged particles and the ambient particles, the DBD plasma actuators act as a jet along the actuator surface. As shown in Figure 3, the maximal induced jet velocity is up to 8 m/s measured at 20 mm away from the

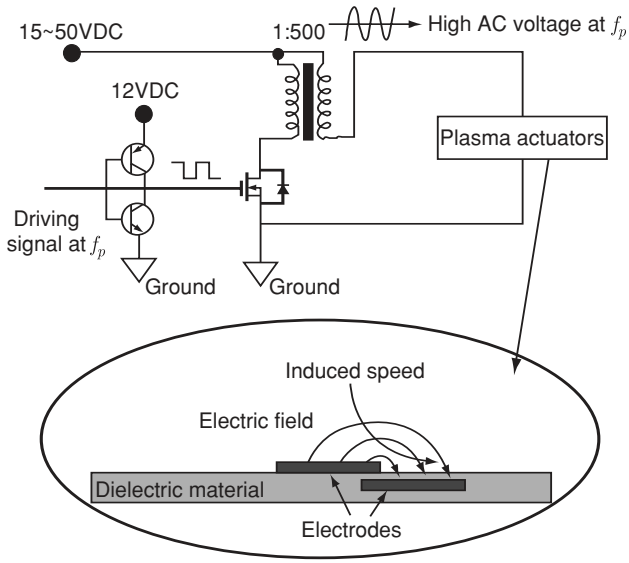

Figure 2: Schematic of a DBD plasma actuator system using the topology of switching circuits.

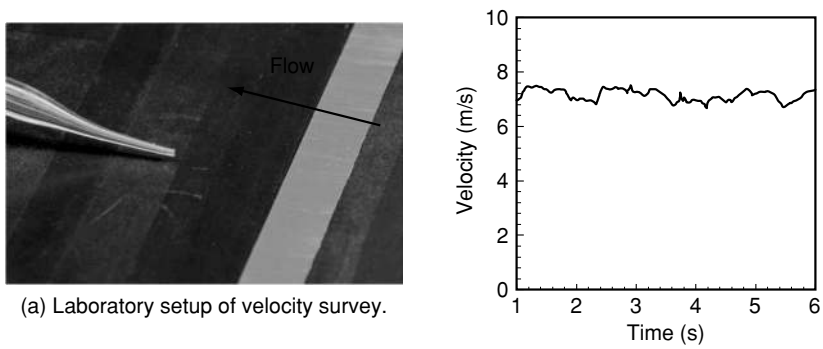

(a) Laboratory setup of velocity survey.

(b) Induced velocity.

Figure 3: Airflow velocity induced by DBD plasma actuators.

electrodes in the direction parallel to the surface (Huang & Zhang, 2008), where the peak-to-peak voltage $V_{pp} = 25$ kV. The measurement was performed approximately 1 mm away from the dielectric surface. The power consumption in this experiment is approximately 5 watts/mm. In theory, a higher velocity of 10 to 15 m/s could be achieved (Shin *et al*., 2007).

A sufficiently high electric field is required to break down the air species to generate atmospheric glow discharges. The power supply shown in Figure 2 has a switching circuit topology that restricts the driving signal to a square wave and the output to a high voltage sinusoid wave. Specially, the driving signal switches a step up transformer through a power metal-oxide-semiconductor field-effect transistor (MOSFET). Two bipolar transistors form a push-pull gate driver to increase the driving ability and reduce the switching loss of the MOSFET devices. The high voltage output of sinusoid waveform is applied to the DBD plasma actuators to sustain the discharges.

As a DBD plasma actuator can be regarded as a capacitive load, the whole DBD plasma system can be viewed an inductance-capacitance (LC) circuit from the electric viewpoint. A DBD plasma system works most efficiently at the oscillation frequency (f_p) of the LC circuit. The value of f_p generally ranges from 3 to 6 kHz for the present actuators. The driving frequency, f_p, could be increased beyond 20 kHz using a suitable impedance matching network (Chen, 2002) to reduce audible noise radiated from the plasma actuators.

The switching-based power system shown in Figure 2 is efficient in energy inversion but can only output a sinusoid wave. This power system has been used in some previous works (Huang *et al*., 2007; Huang *et al*., 2008a). In contrast, the output waveform of a linear amplifier-based power system (see Figure 4) can be sawtooth, square, and sinusoid waveforms. The input waveform generated from a signal generator is linearly amplified to output the high voltage signal with a similar waveform (Roth, 2003; Enloe *et al*., 2004a). The induced body forces from a DBD actuator driven by various waveforms have been compared by Enloe *et al*. (2004b). The comparison shows that the waveform with a positive sawtooth is most optimal. However, up to now the sinusoid waveform is still used for its convenience in most applications.

Figure 5 shows examples of general sinusoid waveforms of voltage (V_p) and current I through a DBD plasma actuator. These can be measured with a high voltage probe. A study on $V_p - I$ curves can help to identify the electric performance of DBD plasma actuators, which is important for design optimization.

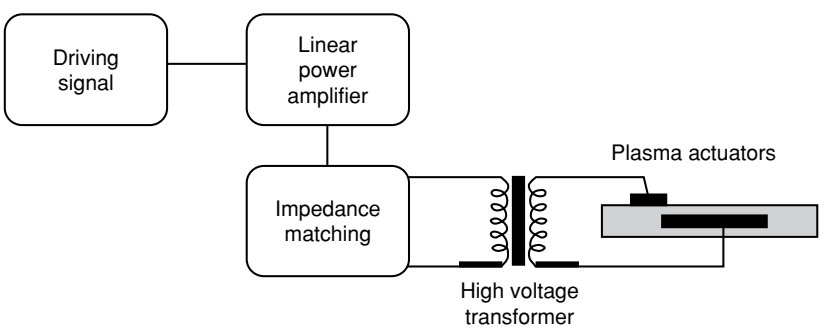

Figure 4: Schematic of a DBD plasma actuator system using the topology of linear circuits.

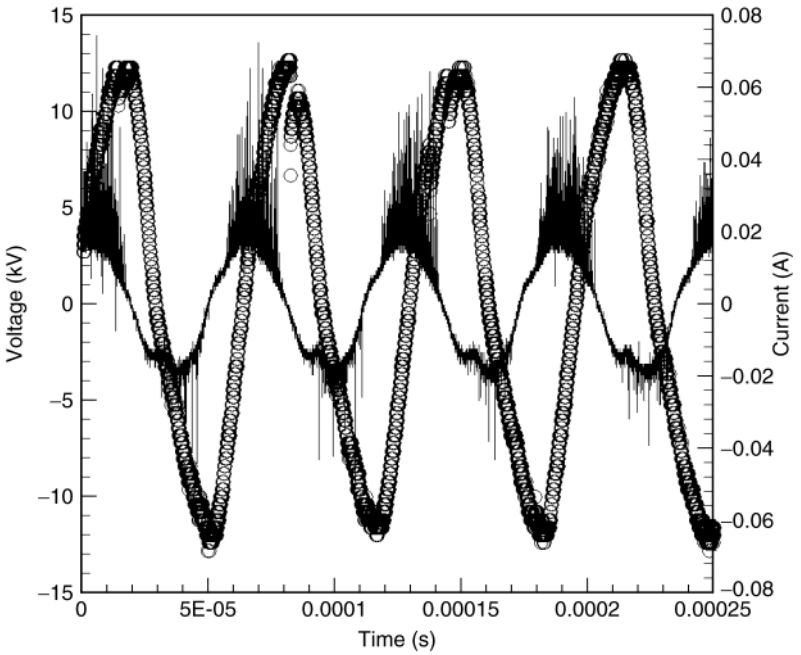

Figure 5: Voltage (o) and current (-) time histories over the actuators (Huang & Zhang, 2008).

3. APPLICATIONS TO FLOW AND NOISE CONTROL

3.1. Cavity flow and noise control

Flow-induced noise radiation from a cavity is a benchmark problem in aeroacoustics (Rossiter, 1964). It has been widely employed in studies of flow-induced noise control (Cattafesta *et al.*, 1999). The problem can be found in many practical applications, such as landing gear bay noise. Figure 6 shows the schematic of a cavity model for wind tunnel tests (Chan, Zhang, & Gabriel, 2007). For cavities of sufficient span, there are different modes of flow oscillation: longitudinal and transverse, depending on the length-to-depth ratio of the cavity and the approaching flow conditions. For a cavity with a length-to-depth ratio larger than one and driven by a sufficiently high Reynolds number flow (turbulent approaching boundary layer), longitudinal modes dominate (Ashcroft *et al.*, 2003). Tonal noise is radiated due to pressure fluctuations within the cavity. Disturbances generated at the leading edge of the cavity are amplified along the shear layer and saturate to form discrete vortical structures. The impingement of these vortical structures on the trailing edge of the cavity produces acoustic waves that propagate in the upstream direction, which reinforce the shedding at the leading edge through a receptivity process. From the classical control perspective a positive feedback loop is formed at these frequencies, where the cumulative increase of the disturbance is finally saturated by the presence of viscous effects.

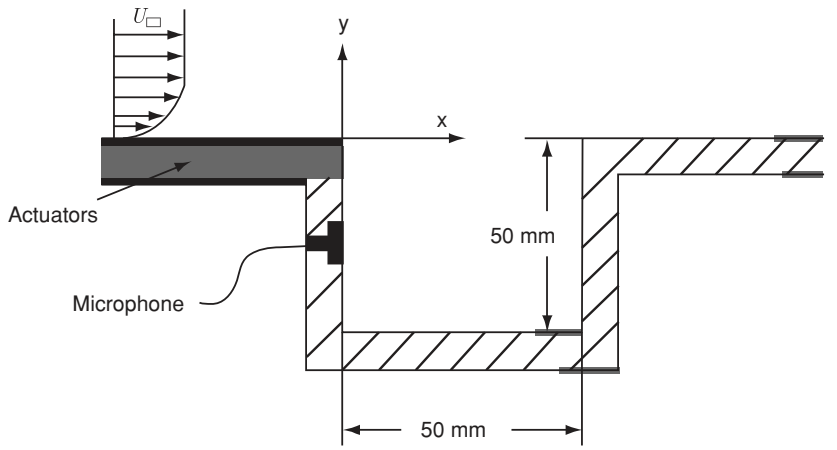

Figure 6: Schematic of cavity model used in noise control tests.

The DBD plasma actuators have been used to attenuate the tonal noise from a cavity (Huang *et al*., 2007, 2008a). The actuators were installed on the approaching surface of the cavity model near the leading edge to control flow disturbances at their initial stage of development.

Figure 7 shows the schematic of a set of typical plasma actuators that act similarly to longitudinal vortex generators (Chan *et al*., 2007). As the direction of electrodes is aligned with the oncoming flow, the actuators are referred to as the streamwise actuators (Huang & Zhang, 2008). In the laboratory test reported by Chan, Zhang, & Gabriel (2007), PIV was used to visualize the shear flow field spanning the opening of the cavity. Sample results are shown in Figure 8. In Figure 8(a), it can be seen that the streamwise velocity distribution experiences small variations across the span when the DBD plasma actuators are not activated. In contrast, Figure 8(b) shows distinctive spanwise velocity variations. Each velocity variance coincides with one electrode of the DBD actuators. Figure 9 shows the outcome of an open-loop control system application. The dominant tone is seen to be attenuated.

A number of possible active flow control approaches for cavity noise attenuation have been summarized by Rowley & Williams (2006), which include a) affecting the boundary layer/shear layer thickness to change hydrodynamic stability characteristics, b) introducing disturbances at off-resonant frequencies to impede the natural resonance and c) shifting the reattachment location of the shear layer on the cavity's trailing wall to interrupt/reduce the acoustic feedback. In the example above, it can be seen that the plasma actuators not only provide an actuation at an off-resonance frequency (3.2 kHz in this case) but also manipulated the shear layer extensively. The disturbances are consequently amplified in the shear layer at different rates, and more importantly, at different phases that can offset each other. The three-dimensional disturbances introduced into the shear layer impede the development of organized structures in the

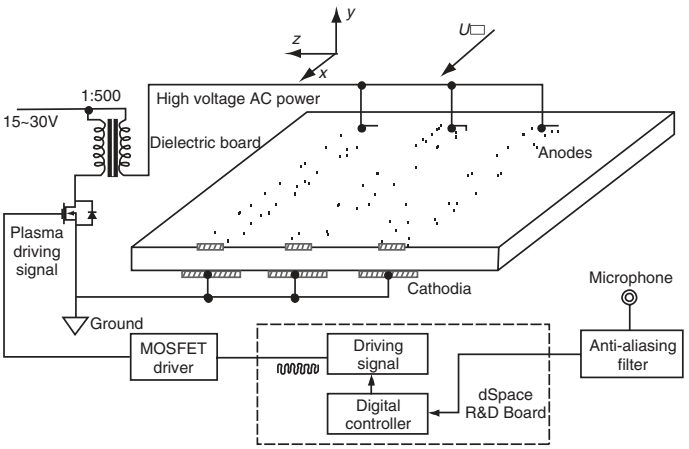

(a) Plasma actuators aligned with flow for cavity noise control.

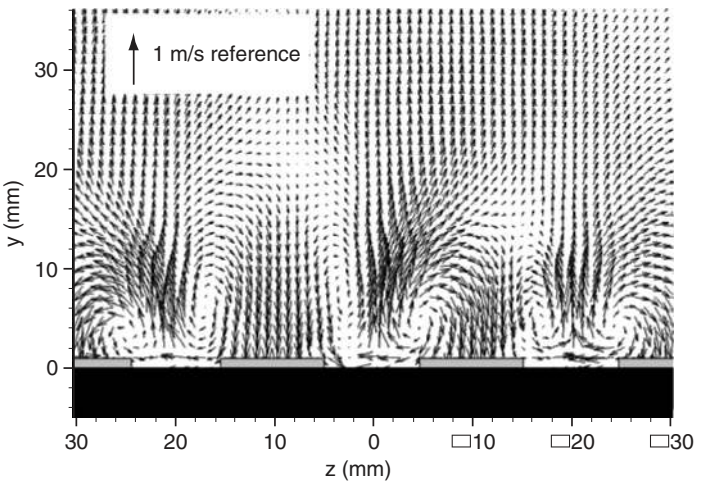

(b) Streamwise vortices induced by the plasma actuators at $U_\infty = 0\frac{m}{s}$.

Figure 7: Plasma actuators for cavity noise control (Chan *et al*., 2007).

cavity shear layer thus disrupting the feedback mechanism that was needed to sustain the fluid-acoustic process. The outcome is the complete attenuation of the tonal noise at the dominant frequency (1043 Hz). For the case shown the system generates a peak-to-peak voltage of V_{pp} = 15 kV and the power consumption is 45 watts.

To improve the control efficiency, the plasma actuators can be integrated into a closed-loop control system. To arrive at a closed-loop system, it is necessary to develop either a linear (Rowley *et al*., 2006) or a nonlinear (Samimy, *et al*., 2007b) model of the cavity system under control (Williams & Rowley, 2006) with plasma actuators, by

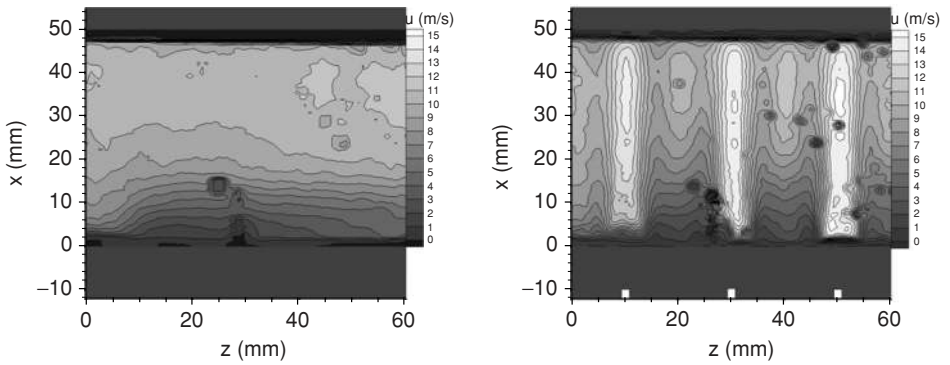

Figure 8: Mean streamwise velocity over the openning of cavity generated by streamwise aligned actuators; flow from bottom to top, $U_\infty = 20\frac{m}{s}$ (Huang & Zhang, 2008).

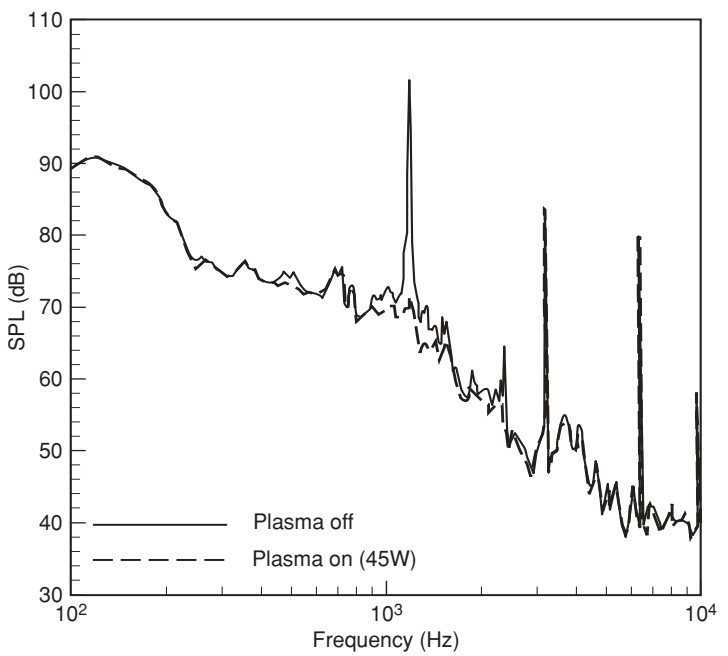

Figure 9: Open-loop cacvity noise control with plasma actuators; $U_\infty = 20\frac{m}{s}$ (Huang *et al*., 2008a).

which the fundamental properties (*e.g.* stability) of the proposed closed-loop control system can be assessed. Control methodologies for a linear model have already been well developed within the control system community. To apply linear control analysis and design techniques, a linear model is generally preferred. For instance, a linearly approximated model, instead of the nonlinear state space model, was used to design a linear quadratic regulator (Samimy *et al*., 2007b). In addition, the attenuation of cavity oscillations by changing the three-dimensional flow field resembles a variable structure process. Figure 10 shows a possible closed-loop scheme with a tentative variable structure that models the plasma effects. The physics-based linear model (Rowley *et al*., 2006) is employed while the inner shear layer model is variable with the plasma actuators.

The linear model is capable of predicting cavity dynamics using several linear transfer functions: the shear layer dynamics, $G(s)$; the acoustic feedback, $A(s)$; scattering gain (K_s) at the trailing edge and receptivity gain (K_r) at the leading edge of a cavity, where s is a complex parameter associated with the Laplace transform, and K_r and K_s are assumed to be constants (Rowley *et al*., 2006; Yan *et al*., 2006). It was suggested that the damping ratio of a cavity system is controlled by the plasma actuator proportionally to the supplied input voltage, V_{DC}, where V_{DC} is the low DC voltage, which is the input of an inverter circuit that produces a high AC voltage to drive plasma actuators (Huang *et al*., 2008a). The amplification rate of the inverter is about 500. The peak-to-peak voltage V_{pp} of the related high AC voltage is 15 kV for V_{DC} = 30 volts (Huang *et al*., 2008a).

The peak amplitudes of the dominant tonal noise associated with V_{DC} have been predicted using the variable structure model (Huang *et al*., 2008a). The effect of the

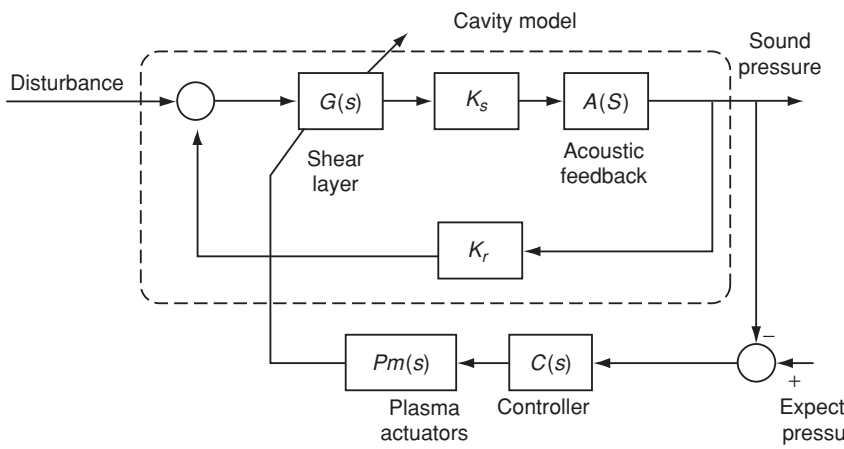

Figure 10: Closed-loop control system with a variable control model (Huang *et al*., 2008a).

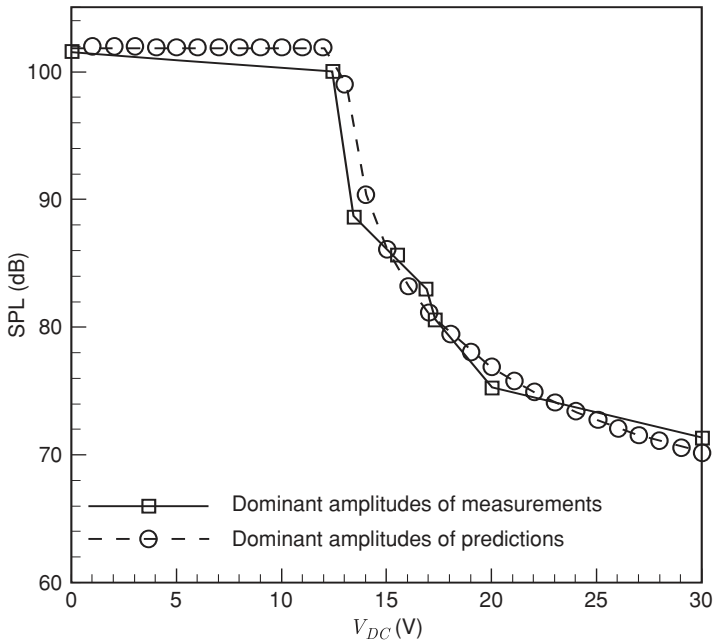

Figure 11: Dominant amplitudes of the measured and the predicted tonal noise against the input low DC voltages; $U_\infty = 20\frac{m}{s}$ (Huang *et al*., 2008a).

plasma actuation was modelled and the modeling results were compared with the measured data in Figure 11. The predictions are shown to match the measured data well. It confirms the assertion that, from the perspective of control, the damping ratio of a cavity system is controlled by the plasma actuator proportionally to the supplied input voltage V_{DC}.

As the variable structure model represents the noise attenuation satisfactorily, a closed-loop controller was designed and implemented on a dSPACE real-time system (Huang *et al*., 2008a). Figure 12 shows the instantaneous sound pressure and the corresponding plasma driving signal's duty cycle. The sound pressure signal was measured by a microphone at the leading edge of the cavity and converted by an ADC on the dSPACE real-time system. The duty cycle of the control signal is 0% when the plasma actuator is switched off; it is 70% when the plasma actuator keeps working; the cycle is varied on-line when the closed-loop control method is applied. The average sound pressure amplitudes are reduced by using both plasma driving signals. When the plasma actuator keeps working, however, it radiates tonal noises with relatively high amplitudes at the harmonic frequencies of the plasma driving signal. An advantage of using the closed-loop control system is that the amplitude of the plasma radiated noise is significantly reduced.

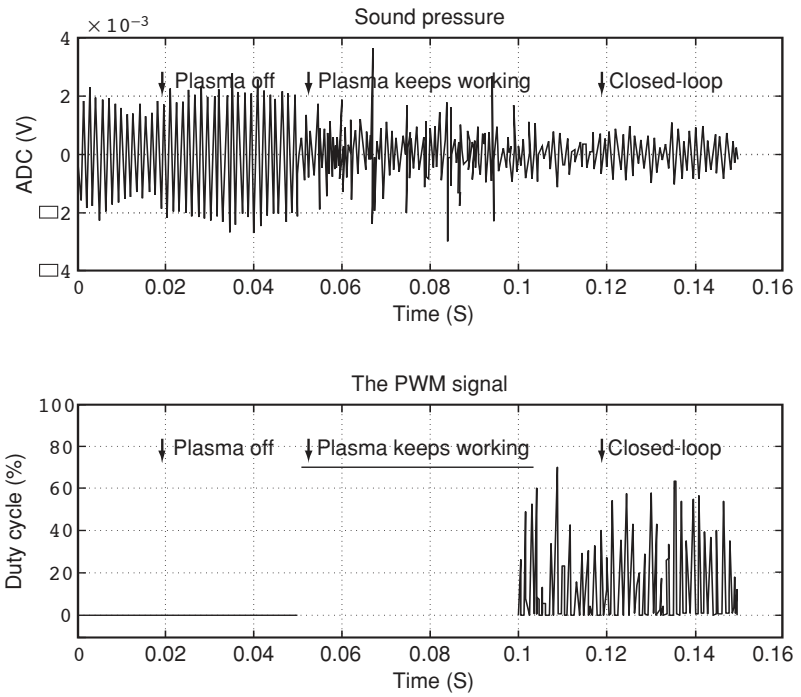

Figure 12: (a) Measured sound pressure at the leading edge of the cavity and (b) the corresponding duty cycle of the plasma driving signal pulse width modulation signal) at U_∞ = 15 m/s (Huang *et al*., 2008a).

3.2. Cylinder flow and noise control

Plasma actuators have been used to control flow around and noise generated by cylinders. In Thomas *et al*. (2008), the Reynolds number with respect to the radius D was 3.3×10^4. The three-dimensional effect of the flow field along the span of the cylinder was omitted. The installation of the plasma actuators on the cylinder was similar to Figure 13(a), which induced a flow directed downstream. The primary objective of the setup was to suppress vortex shedding by maintaining flow attachment over the surface of the lee side of the cylinder with the Coanda effect. The noise control effect over a cylinder wake at U_∞ = 4 m/s was studied by comparing the power spectral density of the near-field pressure fluctuations measured with a microphone that was flush mounted in the wind-tunnel wall. The spectral peak associated with the Karman vortex shedding frequency was completely suppressed using downstream directed actuation. Although it was documented that the near-field sound pressure levels (SPL) at the shedding frequency was reduced by 13 dB (Thomas *et al*., 2008), the fluctuating pressure measured at the microphone could contain contributions from the cylinder wake, the tunnel wall boundary layer,

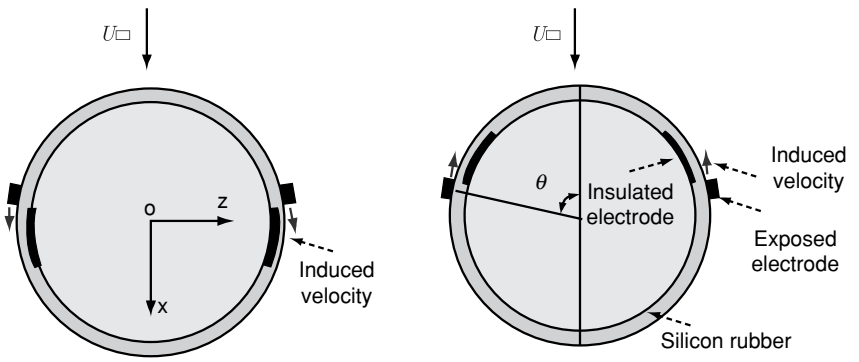

Figure 13: Schematics of plasma actuators on a cylinder.

and downstream fan noise. A far-field measurement should be helpful to validate the control performance.

An investigation of cylinder noise control by plasma actuators was conducted in the University of Southampton, at a freestream speed of 20 m/s. The Reynolds number is 2.1×10^5 based on the cylinder radius D of 100 mm. The length of the cylinder is 500 mm. In addition, the control performance of two types of plasma actuators is compared in the experiments. The setup configuration is shown in Figure 13, where the dielectric constant of the silicon rubber covering the cylinder is 4.7 ± 0.5. Both plasma actuator configurations in Figure 13 induce velocities tangentially along the cylinder surface, one in the generally upstream direction, while the other in the generally downstream direction.

It has been found that the induced speed can oscillate between ± 0.1 m/s at the driving frequency (Moreau *et al.*, 2007). The equivalent actuation on the adjacent fluid could be considered constant, as the characteristic time scale of the oscillation is much smaller than the corresponding scales for the background flow.

Both flow and acoustic experiments have been performed in the Southampton DARP anechoic facility to identify the control effect. Figure 14 shows the test setup. The usable space of the chamber is $7.33 \text{ m} \times 7.33 \text{ m} \times 5.50 \text{ m}$. A nozzle (500 mm × 350 mm) connecting to a plenum chamber can produce a jet flow at a speed of $U_\infty = 20 \pm 0.5$ m/s. The single cylinder model is installed 300 mm downstream of the nozzle exit. The influence of the electric discharge on the adjacent flow field is investigated using a PIV system configured similarly to the cavity experiments discussed in section 3.1. A microphone arc located at about 20D away from the model is used to hold eight BEHRINGER omnidirectional measurement condenser microphones (ECM8000) to measure the far-field sound field. The microphones have a good linear frequency response and omnidirectional polar pattern that help to ensure the quality of the measurements. The lowest sensitive frequency is 15 Hz and the highest one is 20 kHz. The observation angle (defined from the flow direction) with respect to the origin point

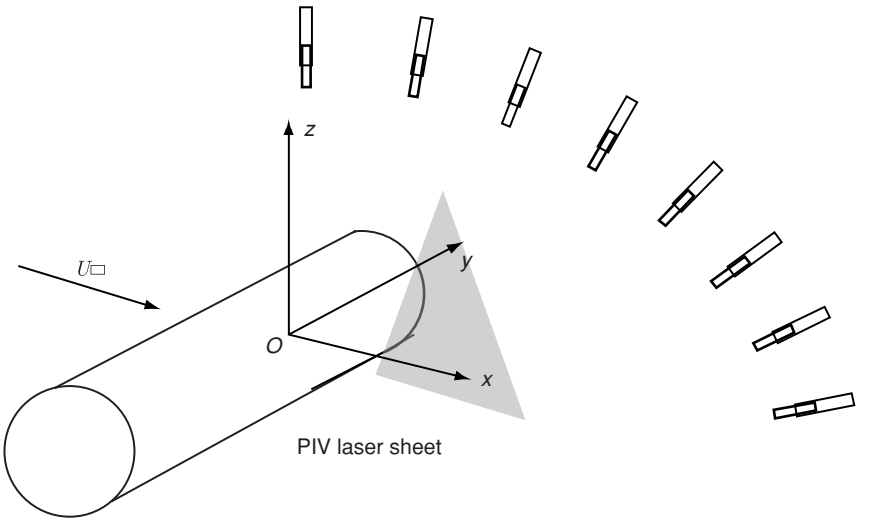

Figure 14: Cylinder noise control in the Southampton DARP anechoic camber.

on the cylinder model ranges from 20 deg to 90 deg. The voltage signals from the microphones are firstly passed through preamplifiers and anti-aliasing filters, and are subsequently sampled at 44.1 KHz. The signal cables and electric circuits are shielded to prevent potential electromagnetic interference from the glow discharges. A 4096 point fast Fourier transform with a Hanning window function is applied to the sampled data. The spectral results are averaged over 100 signal blocks for statistical confidence.

Figure 15 shows the mean u velocity in the x-z plane, where the velocity u is in the x direction. As the model was illuminated from the left by the PIV laser, part of the flow area behind the cylinder could not be visualized. The area is excluded by a gray colored polygon in the figure. Compared to the flow field without plasma actuation, the downstream directed forcing actuation can reduce the width of the wake, while the upstream directed forcing actuation increases the width of the wake. It shows that the wake width is reduced by 8% with the downstream directed actuation at x = 75 mm at a freestream speed of U_∞ = 20 m/s, while the upstream directed actuation increases the width by 7%. This finding is compatible with the physical intuition as well as results reported elsewhere (Sung *et al*., 2006).

Figure 16 shows that the plasma actuators with the upstream directed forcing actuation work more efficiently than those producing the downstream directed forcing. There is almost a 1.5 ± 0.5 dB noise reduction in the frequency range between 100 Hz and 3 kHz by the upstream directed actuation. The maximal noise reduction is almost 3 dB near 2500 Hz. In contrast, the noise reduction with the downstream directed actuation is limited. Compared to previous works (Thomas *et al*., 2008) the background noise of the jet flow from the high pressure plenum chamber dominates the low frequency spectrum at 20 m/s. As a result the strong tonal noise due to the vortex

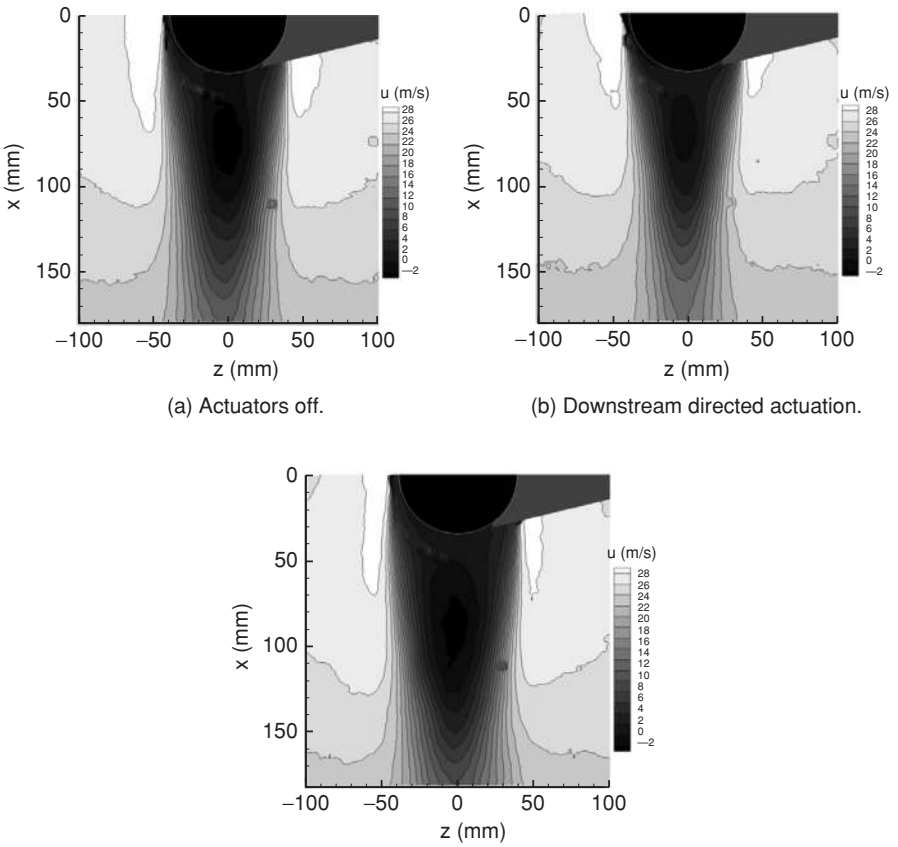

(a) Actuators off.

(b) Downstream directed actuation.

(c) Upstream directed actuation.

Figure 15: Mean streamwise velocity around the cylinder; flow from top to bottom.

shedding at low frequency (<100 Hz) is not discovered in the present investigation. On the other hand, distinctive noise increases at the plasma driving frequency and its harmonics can be found in Figure 16. This unfavorable noise radiating from the plasma system can be avoided by increasing the driving frequency beyond the human hearing threshold.

3.3. Bluff body flow and noise control

In the area of aircraft noise control, bluff bodies appear on landing gears and normally consist of cylinders installed with struts. An example of bluff body noise control (Huang *et al*., 2008) uses a 1/4 scale model representing a low main strut installed on a landing gear, consisting of a cylinder and a torque link component. The torque link is installed on the downstream side of the cylinder, formed by two triangle shaped plates at an angle $\alpha = 90$ deg (see Figure 17).

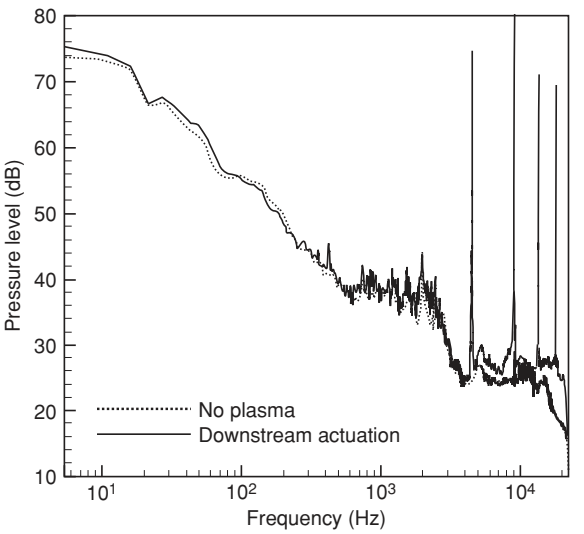

(a) Downstream directed actuation.

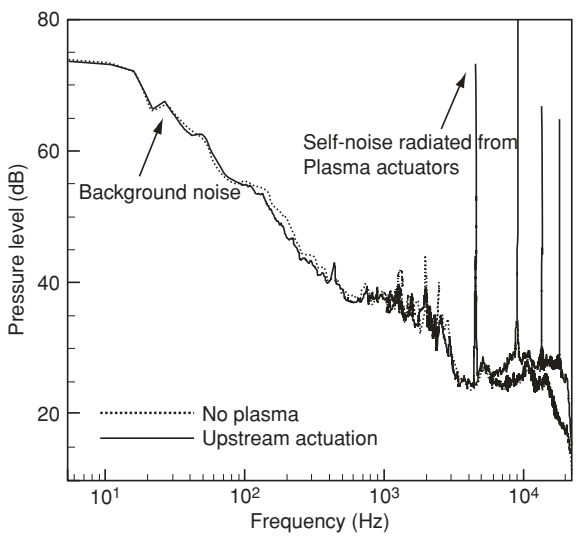

(b) Upstream directed actuation.

Figure 16: SPL values of the cylinder case at $U_\infty = 20$ m/s.

The noise radiating from the model is higher at broadband frequencies compared to a single cylinder model (Sung *et al*., 2006; Forte *et al*., 2007). This increase is thought to be caused by the flow-structure interaction between the cylinder wake and the torque link. Figure 18(a) shows a schematic of the plasma actuators installed on the surface of the cylinder. The thick black curves denote the electrodes made by

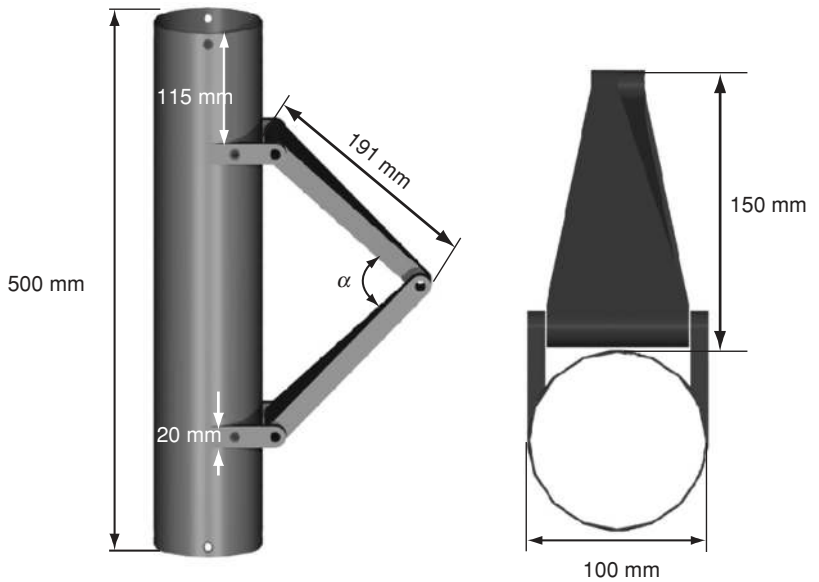

Figure 17: Schematic of bluff body test model (Huang *et al.*, 2008b).

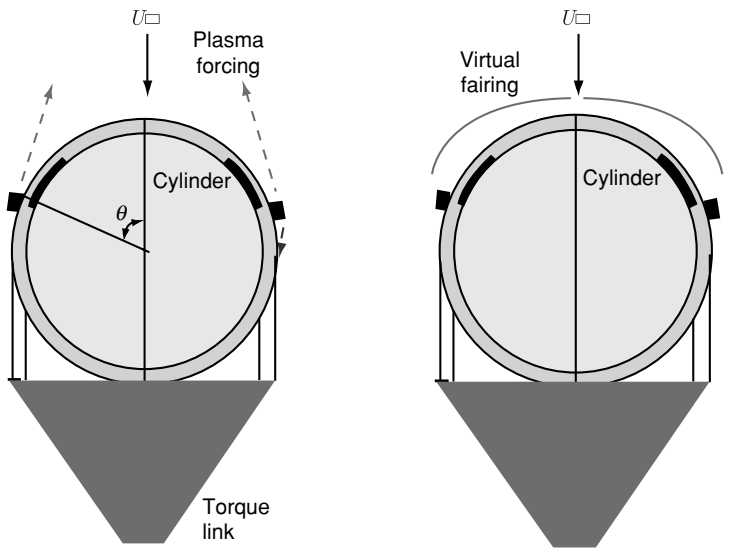

(a) Schematic of upstream directed actuation. (b) The effect of upstream actuation.

Figure 18: Schematic of the plasma actuators installed on the surface of the bluff body model.

copper tapes of thickness 0.04 mm. The width of the electrodes exposed to air is 10 mm. The width of the electrodes insulated by the dielectric material is 20 mm. Both parameters are selected empirically. The total spanwise length of the plasma actuators is 350 mm, which is consistent with the size of the test section of the Southampton DARP anechoic chamber. Silicon rubber of thickness 1 mm is the dielectric material (dielectric constant of 6.5± 1).

The exposed electrodes in Figure 18 are connected to a high voltage alternating current (AC) power supply. The power supply is similar to that shown in Figure 2. The insulated electrodes are grounded. To sustain the discharges, the AC voltage for the current system operates at a frequency on the order of kHz. The peak-to-peak voltage is 25 kV and the overall power consumption is about 200 watts. The plasma actuators in Figure 18(a) induce a speed in the generally upstream direction. The exposed electrodes for the upstream directed actuators are placed at $\theta = \pm 80$ deg to the upstream. The PIV results in Figure 15 for an isolated cylinder already suggest that the upstream directed actuation is able to increase the width of the wake, which could reduce the interaction between the cylinder wake and the downstream torque link. The upstream directed actuators therefore act as a fairing before the bluff body (see Figure 18 (b)). Downstream directed actuators placed at $\theta = \pm 50$ deg are tested separately to compare the control performance. Although plasma actuation applied at bifurcation points at $|\theta| > 80$ deg may be more effective for flow manipulation, there is a risk of an electric breakdown between the exposed electrodes and the metal torque link if the two parts are too close.

It is worthwhile to mention that a jet normal to the cylinder surface can be produced if both the upstream and downstream directed actuators are activated simultaneously. However, little control performance was found in the experiments using this normal jet actuation. The following discussion is therefore limited to the upstream directed and downstream directed actuators working in a steady mode. As the dominant noise for the bluff body case is presumably caused by the interaction between the cylinder wake and the downstream torque link, affecting large-scale structures in the cylinder wake extensively is preferable. The change of large-scale structures can reduce broadband noise by cascading effects. Compared to the steady actuation, the unsteady actuation is inefficient in controlling large-scale structures for its reduced authority. The unsteady actuation may still work by inducing perturbations, canceling the disturbances originally shed from the cylinder or the torque link. However, similar to the aforementioned cavity case, a control model is required to keep the perturbations and disturbances out of phase. The steady actuation is only used here in absence of a control model for the bluff body case.

For the bluff body noise control, the effectiveness of the plasma actuators is again examined at a speed of 30 m/s. The corresponding Reynolds numbers based on the cylinder diameter D is 2.1×10^5. Figure 19 shows the setup of the experiment. The time-mean flow is visualized using PIV in the x-z plane at approximately $y = 0$ mm. However, it is difficult to visualize the dynamics of flow field between the cylinder and the torque link using a PIV system. The study is therefore focused on acoustic

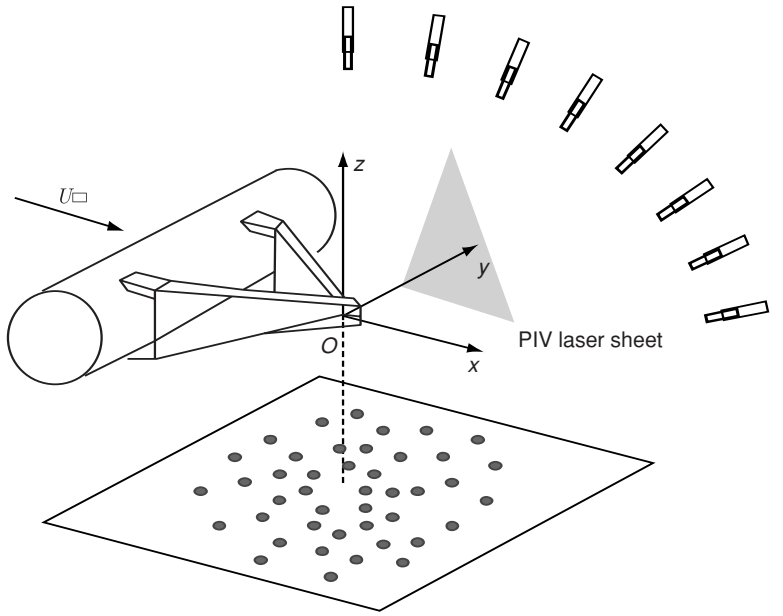

Figure 19: Bluff body noise control in the Southampton DARP anechoic camber.

experiments. The near-field noise sources are located by an microphone array with 56 microphones. The conventional beamforming technique is adopted to produce the acoustic images of sound (Mueller, 2002). The diameter of the array is 0.64 m. An arc containing eight microphones located at a distance of 20D away from the model is used to measure the far-field sound.

Figure 20 shows some acoustic images at 5 kHz in dB. The sound pressure level (SPL) for all three figures have been non-dimensionalized by the maximal SPL value measured without plasma actuation. It can be seen that the SPL of the dominant source around the torque link joint is reduced by up to 3.5 ± 0.3 dB at a freestream velocity of 30 m/s. The performance of the upstream directed actuators is better than that of the downstream directed actuators. Similar findings were found for acoustic images computed at other frequencies.

Figure 21 compares the SPL results over broadband frequencies at 30 m/s. The results from all eight far-field microphones are averaged to show collective control effects. It is worthwhile mentioning that the results from any single microphone are quite similar. It can be observed the tonal noise from the cylinder at the shedding frequency is overwhelmed by the background noise. On the other hand, it can be seen that the upstream directed actuation attenuates noise more effectively, especially at the

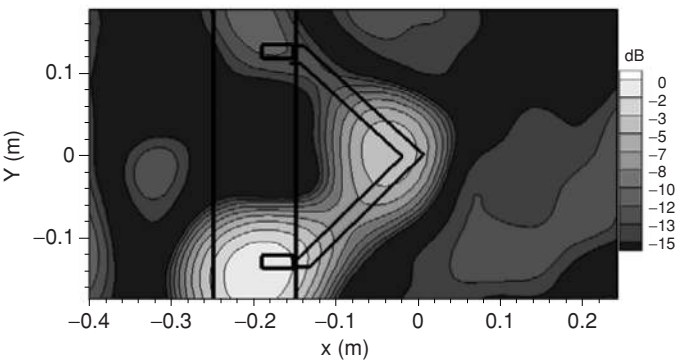

(a) Actuators off.

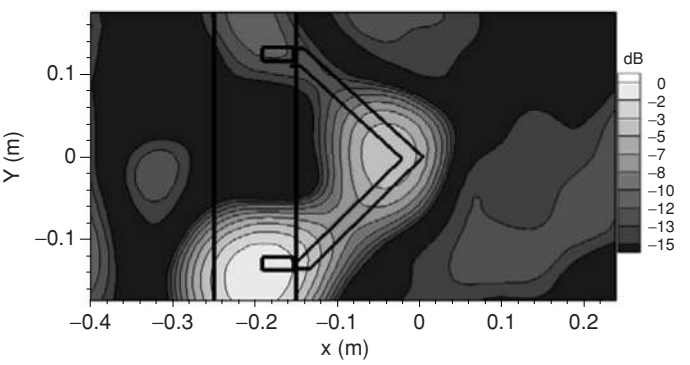

(b) Upstream directed actuation.

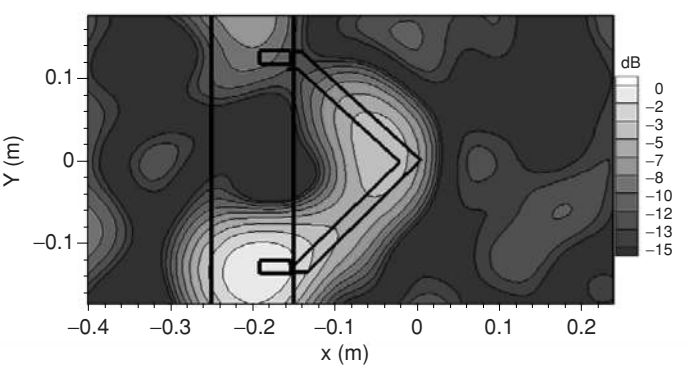

(c) Downstream directed actuation.

Figure 20: Acoustic images at $f = B$ kHz, $U_\infty = 30$ m/s, $z = 0$ (Huang *et al.*, 2008b).

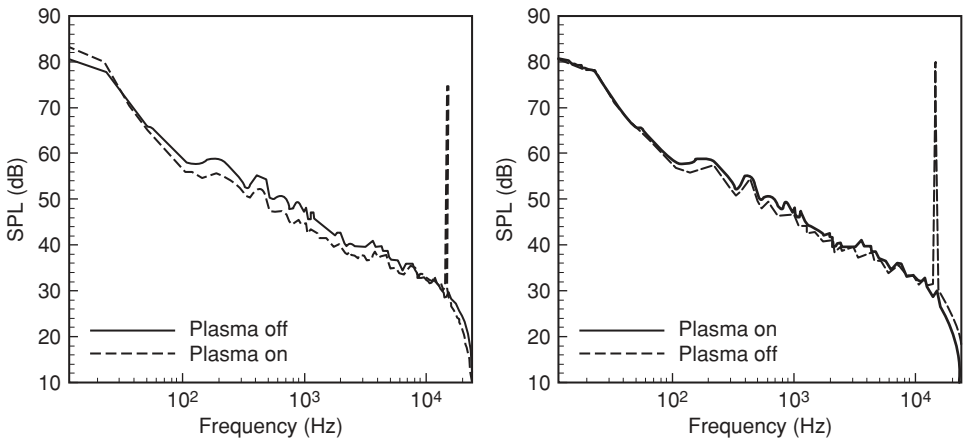

Figure 21: Far-field SPL of the bluff body case at $U_\infty = 30$ m/s.

frequency ranges from 1 kHz to 3 kHz. There is up to 3± 0.2 dB reduction with the upstream directed actuation; whilst up to 1.7± 0.2 dB reduction with the downstream directed actuation. The noise control effectiveness is reduced at higher frequencies due to the interference from the self-noise of the plasma actuators, which is especially dominant at the working frequency of $f_p = 15$ kHz.

4. SUMMARY

The stringent targets set by the Advisory Council for Aerospace Research in Europe (ACARE) aim at a reduction of perceived external noise radiation by civil aircraft of up to 50% by 2020. This target cannot be met by conventional research and development circle alone. New operation procedures and ATM, and novel noise control methods/technologies need to be developed. The technique discussed in this article follows the tradition of Professor Geoffrey Lilley's work at Southampton. It represents a new method but worthy of research and development. Some advantages of the methods are simplicity, absence of mechanical moving parts, and fast response. Examples considered in this article include the attenuation of a cavity oscillation, a cylinder noise control, and a bluff body noise control applications, which demonstrate that the method can be used to attenuate both tonal and more importantly broadband noise radiated by components typically found on an aircraft. However, it worthwhile mentioning that these cases were all conducted at relatively low Reynolds number. The noise control effectiveness of DBD plasma actuators deteriorates as the Reynolds number is increased. This discovery reflects the stringent open problem of low authority (control performance) of the existing plasma actuators, which call for further investigation.

REFERENCES

Ashcroft, G., Takeda, K., & Zhang, X. (2003). A numerical investigation of noise

radiated by a turbulent flow over a cavity. *Journal of Sound and Vibration, 265* (1), 43–60.

Cattafesta, L. N., Shukla, D., Garg, S., & Ross, J. A. (1999). *Development of an adaptive weapons-bay suppression system*. AIAA paper 1999-1901.

Chan, S., Zhang, X., & Gabriel, S. B. (2007). The attenuation of cavity tones using plasma actuators. *AIAA Journal, 45* (7), 1525–1538.

Chen, Z. Y. (2002). Impedance matching for one atmosphere uniform glow discharge plasma (OAUGDP) reactors. *IEEE transcation on Plasma Science, 30* (5), 1922–1930.

Curle, N. (1955). The influence of solid boundaries upon aerodynamic sound. *Proceedings of the Royal Society London, A231* (1187), 505–514.

Elias, P. Q., Chanetz, B., Larigaldie, S., & Packan, D. (2007). Study of the effect of glow discharges near a M=3 bow shock. *AIAA Journal, 45* (9), 2237–2245.

Enloe, C. L., McLaughlin, T. E., Van Dyken, R. D., Kachner, K. D., Jumper, E. J., & Corke, T. C. (2004b). Mechanisms and responses of a single dielectric barrier plasma actuator: plasma morphology. *AIAA Journal, 42* (3), 589–594.

Enloe, C. L., Mclaughlin, T. E., Van Dyken, R. D., Kachner, K. D., Jumper, E. J., Corke, T. C., et al. (2004a). Mechanisms and responses of a dielectric barrier plasma actuator: geometric effects. *AIAA Journal, 42* (3), 595–604.

Forte, M., Jolibois, J., Pons, J., Moreau, E., Touchard, G., & Gazalens, M. (2007). Optimization of a dielectric barrier discharge actuator Optimization of a dielectric barrier discharge actuator by stationary and non-stationary measurements of the induced flow velocity: application to airflow control. *Experiments in Fluids, 43* (6), 917–928.

Gnemmi, P., Charon, R., Duperoux, J. P., & George, A. (2008). Feasibility study for steering a supersonic projectile by a plasma actuator. *AIAA Journal, 46* (6), 1308–1317.

Greenblatt, D., Goksel, B., Rechenberg, I., Schule, C. Y., Romann, D., & Paschereit, C. O. (2008). Dielectric barrier discharge flow control at very low flight Reynolds numbers. *AIAA Journal, 46* (6), 1528–1541.

Huang, X., & Zhang, X. (2008). Streamwise and spanwise plasma actuators for flow-induced cavity noise control. *Physics of Fluids, 20* (3), 037101 DOI:10.1063/1.2890448.

Huang, X., Chan, S., & Zhang, X. (2007). An atmospheric plasma actuator for aeroacoustic applications. *IEEE Transcations on Plasma Science, 35* (3), 693–695.

Huang, X., Chan, S., Zhang, X., & Gabriel, S. B. (2008a). Variable structure model for flow-induced tonal noise control with plasma actuators. *AIAA Journal, 46* (1), 241–250.

Huang, X., Zhang, X., & Gabriel, S. B. (2008b). *Bluff body noise and flow control with atmospheric plasma actuators*. AIAA paper 2008-3044.

Kim, J. H., Kastner, J., & Samimy, M. (2009). Active control of a high Reynolds number Mach 0.9 axisymmetric jet. *AIAA Journal, 47* (1), 116–128.

Leonov, S., Bityurin, V., & Yarantsev, V. (2003). *The effect of plasma induced separation*. AIAA 2003-3853.

Moreau, E., Leger, L., & Touchard, G. (2006). Effect of a DC surface non-thermal plasma on a flat plate boundary layer for airflow velocity up to 25 m/s. *Journal of Electrostatics, 64*, 215–225.

Moreau, E., Louste, C., & Touchard, G. (2007). Electric wind induced by sliding discharge in air at atmospheric pressure. *Journal of Electroostatics, 66* (1–2), 107–114.

Mueller, T. J. (Ed.). (2002). *Aeroacoustic measurements*, Springer.

Raman, G., & McLaughlin, D. K. (2000). Recent aeroacoustics research in the United States. *Noise & Vibration Worldwide, 31* (10), 15–20.

Rossister J. E., (1964). Wind-Tunnel Experiments on the Flow over Rectangular Cavities at Subsonic and Transonic Speeds, Aeronautical Research Council Report Memo 3438.

Roth, J. R. (2003). Aerodynamic flow acceleration using paraelectric and peristaltic electrohydrodynamic effects of a one atmosphere uniform glow discharge plasma (OAUGDP). *Physics of Plasmas, 10* (5), 1166–1172.

Roth, J. R. (1998). Electrohydrodynamically induced airflow in a one atmosphere uniform glow discharge surface plasma. *Proceedings of the 25th IEEE International Conference on Plasma Science*, (pp. 6P–67). Raleigh, North Carolina, USA.

Roth, J. R., Sherman, D. M., & Wilkinson, S. P. (2000). Electrohydrodynamic flow control with a glow-discharge surface plasma. *AIAA Journal, 38* (7), 1166–1172.

Rowley, C. W., & Williams, D. R. (2006). Dynamics and control of high-Reynolds-number flow over open cavities. *Annual Review of Fluid Mechanics, 38*, 251–276.

Rowley, C. W., Williams, D. R., Colonius, T., Murray, R. M., & MacMynowski, D. G. (2006). Linear models for control of cavity flow oscillations. *Journal of Fluid Mechanics, 547*, 317–330.

Samimy, M., Debiasi, M., Caraballo, E., Serrani, A., Yuan, X., Little, J., *et al*. (2007b). Feedback control of subsonic cavity flows using reduced-order models. *Journal of Fluid Mechanics, 579*, 315–346.

Samimy, M., Kim, J. H., Kastner, J., Adamovich, I., & Utkin, Y. (2007a). Active control of high-speed and high-Reynolds-number jets using plasma actuators. *Journal of Fluid Mechanics, 578*, 305–330.

Shin, J., Narayanaswamy, V., Raja, L. L., & Clemens, N. T. (2007). Characterization of a direct-current glow discharge plasma actuator in low-pressure supersonic flow. *AIAA Journal, 45* (7), 1596–1605.

Sung, Y., Kim, W., Mungal, M. G., & Cappelli, M. A. (2006). Aerodynamic

modification of flow over bluff objects by plasma actuation. *Experiments in Fluids, 41*, 479–486.

Thomas, O. F., Kozlov, A., & Corke, C. T. (2008). Plasma actuators for landing gear noise reduction. *AIAA Journal, 46* (8), 1921–1931.

Utkin, Y. G., Keshav, S., Kim, J. H., Kastner, J., Adamovich, I. V., & Samimy, M. (2007). Development and use of localized arc filament plasma actuators for high-speed flow control. *Journal of Physics D: Applied Physiscs, 40*, 685–694.

Williams, D. R., & Rowley, C. W. (2006). *Recent progress in closed-loop control of cavity tones*. AIAA paper 2006-0712.

Yan, P., Debiasi, M., Yuan, X., Little, J., Ozbay, H., & Sammimy, M. (2006). Experimental study of linear closed-loop control of subsonic cavity flow. *AIAA Journal, 44* (5), 929–938.